UNIVERSITY OF CALIFORNIA
SANTA CRUZ

SYNTHESIS OF A CATIONIC INORGANIC LAYERED MATERIAL FOR TRAPPING ANIONIC PHARMACEUTICAL POLLUTANTS

A thesis submitted in partial satisfaction
of the requirements for the degree of

MASTERS OF SCIENCE

In

CHEMISTRY

by

Kevin Michael Sergo

September 2013

The thesis of Kevin Michael Sergo is approved:

Professor Scott R.J. Oliver

Professor Pradip K. Mascharak

Professor Yat Li

Tyrus Miller
Vice Provost and Dean of Graduate Studies

Table of Contents

List of Figures

List of Tables

Abstract

Synthesis of a Cationic Inorganic Layered Material for Trapping Pharmaceutical Pollutants

by

Kevin Michael Sergo

A large variety of pharmaceutical classes of drugs (NSAIDs, Beta-blockers, Statins, and others) have been found in aqueous environments at ng/L to μg/L concentrations. While these concentrations are seemingly low in comparison to most of the effective doses for pharmaceuticals, very little is known about chronic low level exposure to these drugs in humans or other animals. Humans will be exposed through their drinking water or bioaccumulation in the food chain. For animals, fish are the main concern for pollutants in an aqueous environment. Millions of people rely on fish heavy diets and could be exposed low levels of a variety of pharmaceuticals by eating. Therefore, it is important to develop materials for sequestering these pollutants. One of the most common methods for pollutant trapping is *via* anion exchange. Most anion exchange mediums are designed for cationic exchange. However, a large amount of these pharmaceutical wastes exist in an anionic form. A variety of materials exhibit anion exchange properties, such as, organically modified resins, layered double hydroxides (LDHs), or metal organic frameworks (MOFs). We are investigating a new class of cationic materials called layered metal hydroxides (LMHs). They consist of cationic inorganic layers balanced by a variety of organic

and inorganic anions. The inorganic layers are exceptionally thermally and chemically stable making them ideal candidates for coupling to raw industrial waste waters. It is highly beneficial to trap the pollution at the source while it is still concentrated, rather than when it has diluted in the environment.

Slug-27 an erbium based LMH with the chemical formula $Er_{12}(OH)_{29}(H_2O)_5(O_3SCH_2CH_2SO_3)_{3.5}\cdot 4H_2O$. The +7 charge in the cationic layer is balanced by 3.5 divalent ethanedisulfonate anions. Full anion exchange for a series of α,ω-dicarboxylates is achieved in a 24 hour period at room temperature and shown by a variety of spectroscopic methods. Slug-27 also exhibits interesting rehydration properties after being heated to temperatures of 200˚ C and greater. Future studies on Slug-27 will include the effect of dehydration/rehydration on the exchange properties.

Dedication

To my parents
for all the love and support
that has allowed me to grow everyday
into something more than I was yesterday

Thank you

Acknowledgement

I would like to acknowledge the following people for their assistance with parts of the research contained in this thesis: Cari Han, Jessica St. John, Yashar Abdollahian, Honghan Fei, and Professor Scott R.J. Oliver.

Introduction

Pharmaceutical products have increased the quality of life and life expectancy across the globe. However, the wastes generated by these drugs are slowly impinging on the environment we rely on to thrive. The EPA more broadly encompasses many of these wastes as Pharmaceuticals and Personal Care Products (PPCPs). These wastes include prescription and over-the-counter drugs, veterinary drugs, fragrances, nutraceuticals (vitamin supplements), cosmetics, sunscreen products and medical diagnostic agents[1]. The fate of these compounds is often an aqueous environment. It is usually the case that they are found in concentrations far lower than the therapeutic dosage (ng/L to µg/L), but almost nothing is known about chronic low-level exposure to these compounds[2,3,4]. Effective and robust water scrubbing techniques need to be studied extensively to ensure clean water for future generations. It is imperative because the industries producing these wastes will continue to grow and introduce these wastes into the environment.

The main route of release for pharmaceutical waste is through the toilet. Hospitals are one of the worst sources for pharmaceutical waste due to the high concentration of people ingesting and excreting drugs. Wastes include many of the regular prescription antibiotics, hormones, etc., but also include specialized contrast agents for medical imaging[3]. Very few, if any, drugs are 100% metabolized, which results in the excess being excreted in either the feces or urine. Metabolites and conjugates of the drug are also excreted along with the parent drug. Sewage is treated for the removal of human

excrement and certain pollutants, but not all are captured. The drugs that pass through treatment plants include analgesics, antibiotics, mood stabilizers, endocrine disrupters, contraceptives, stimulants, tranquilizers, and statins[1-4]. Antibiotics and hormone-based drugs are particularly troubling for a variety of reasons. Low-level or any exposure to antibiotics can lead to bacterial resistance, which will greatly decrease the efficacy of these drugs. Tetracycline (and its derivatives) is a highly used antibiotic in the agriculture industry and pharmaceutically; it has been detected in concentrations as high as 20 mg/kg in topsoil. Rain and/or regular watering can easily cause this to leach into an aqueous environment. Hormone based drugs, or endocrine disrupting compounds, have very low effective doses, so even small amounts in the environment can have a large effect[3]. Low dosages of sex hormones (e.g. estradiol or testosterone) have been shown to induce sex reversal in eggs and larvae. Fish exposed to these hormones often show decreased fecundity through decreased sperm and egg production[5].

Millions of people around the globe rely on very fish heavy diets. If our drugs effect the life cycle of the fish, there could be disastrous consequences for the food web as a whole. Alteration of the life cycle could lead to population collapse and/or the ingestion of the drugs that are in the fish. Population collapse can lead to extreme alterations in the eco-system and food chain. Neonicotinoid pesticides (relatives of nicotine) are highly toxic to bee populations. In controlled studies, these pesticides decrease the production of new Queen Bees in bumble bee colonies by 85%[6]. With a

dramatic decline in the bee population, many plants will not receive the pollination necessary to bear fruits. This lack of pollination will affect both human consumers of those foods, as well as the wild animals that rely on those fruits for sustenance.

Herein, there will be a brief discussion focusing on the wastes generated from the use of a variety of pharmaceutical products and their method of action in the human body. Following this will be a discussion on the various methods used for remediation.

Pharmaceutical pollutants

Non-steroidal anti-inflammatory drugs (NSAIDs) are one of the more common pollutants due to their high volume of use. In both sediment and water samples they have been found in the concentration ranges of ng/g to μg/g and ng/L to μg/L, respectively[7,8]. NSAIDs, such as Naproxen and diclofenac (Fig. 1), are used for treatment of pain and swelling by affecting the COX-1 and COX-2 systems that regulate prostaglandins. Prostaglandins regulate constriction/dilation of vascular smooth muscle, aggregation/disaggregation of platelets, and can induce labor in women among other systems. Rainbow trout have been found to have 83% and 77% homology to the COX-2 and COX-1 proteins in humans[4]. In a low-dose chronic exposure study, it was found that rainbow trout exposed at 5 μg/L of diclofenac for 28 days, renal lesions appeared and the gills were altered[9].

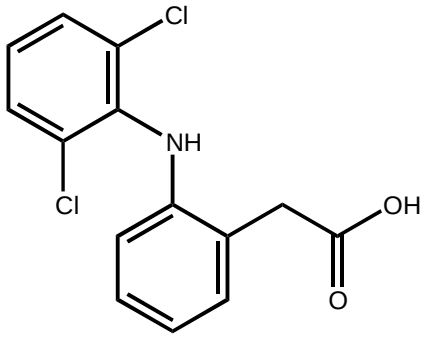

Figure 1. Chemical structure of diclofenac. NSAID marketed under many trade names.

Beta-blockers, which are mainly used to treat hypertension, act in the central nervous system (CNS). They pass through the blood brain barrier and will interact with the adrenergic system. The mis-regulation or unintended regulation of the adrenaline and epinephrine in our body can affect the beating of the heart, vasodilation, and bronchodilation. Propranolol (Fig. 2), one of the first beta-blockers, has been found in US waste water samples at concentrations of 1.9 μg/L. Metabolites of propranolol either excreted in the urine and feces or formed in waste water treatment plants exist in anionic forms. Chronic low-dose exposure to propranolol (0.5-1.0 μg/L over 4 weeks) has shown to decrease the number of eggs released during spawning activities in *O. latipes*[10]. Effecting the reproductive cycles of wild animals will have the greatest effect on their population. Of the thousands of fertilization events that happen during spawning, only a fraction of them will make it to maturity. Reduction in the number of eggs available for fertilization can greatly decrease the population in just one generation.

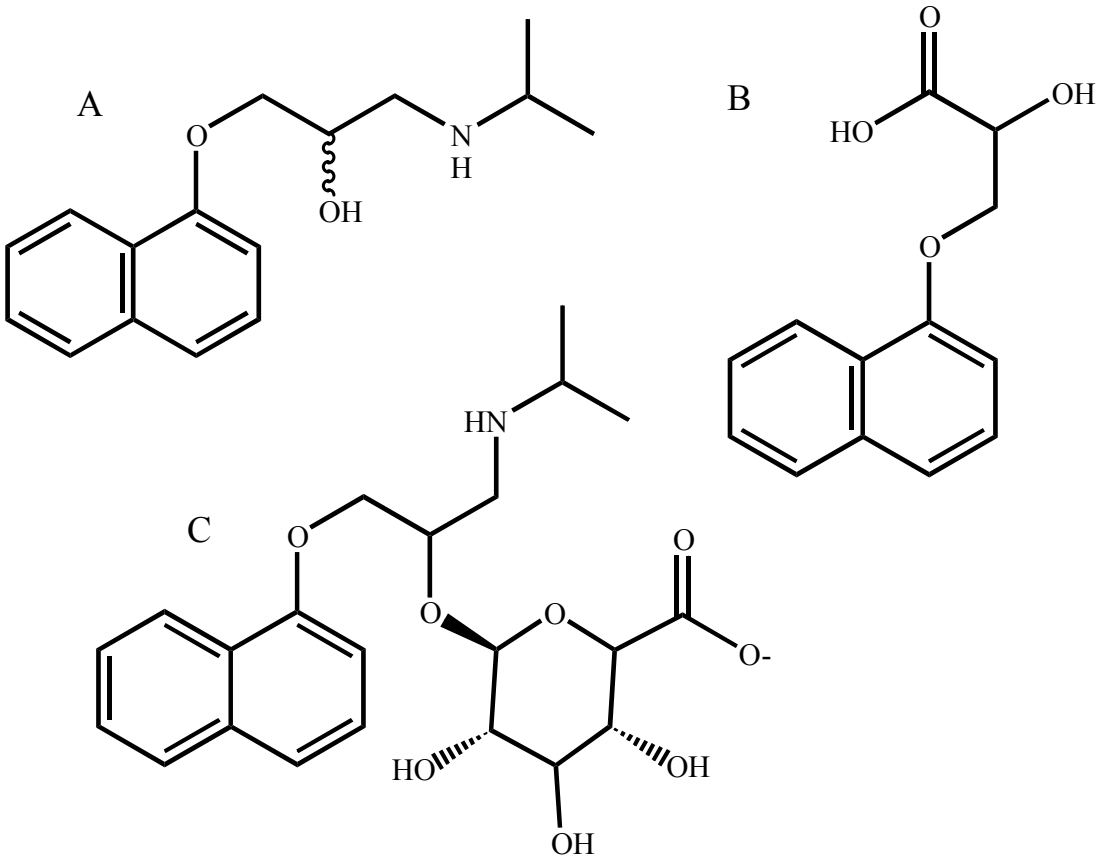

Figure 2. Chemical structure of propranolol (A) with two of its major metabolites, naphthyloxylactic acid (B), and propranolol glucuronide (C). Propranolol is a beta-blocker marketed under many trade names.

Statins regulate cholesterol metabolism by inhibiting HMG CoA reductase from converting HMG CoA to mevalonic acid, which is the first step in the biosynthesis of most lipids[11]. This inhibition causes the expression of LDL receptors on the liver, which ultimately up-regulates the catabolism of lipids in the plasma[12]. Drugs to treat hypercholestoremia (high cholesterol) are some of the most widely prescribed (e.g. Lipitor, largest selling pharmaceutical product in history), and therefore, have the potential to be environmental pollutants. One of the largest concerns is the fact that they have nanomolar affinity for the HMG CoA reductase enzyme. Very low

environmental concentrations can have a legitimate effect due to the low effective concentration. Statins have yet to show real negative effects on their own in the environment, however, it is the interaction between statins and other environmentally relevant pollutants that may lead to trouble for living organisms. Myopathy, a muscle disease, can occur when statins are taken with a drug that may affect statin metabolism, such as fibrates. Fibrates will affect the metabolism of the statin itself, and can therefore lead to several adverse effects such as rhabdomyolysis, the breakdown of damaged skeletal muscle tissue[13].

Neuro-active compounds, such as anti-epileptics and anti-depressants act in the CNS. Many of the anti-depressants are selective serotonin re-uptake inhibitors (SSRIs). Two of which, fluoxetine (trade name Prozac, Figure 3, top) and sertraline (trade name Zoloft, Figure 3, bottom), have been found in wild fish in the US at concentrations of 1.6 ng/g and 4.3 ng/g, respectively[4]. There has been no evidence, as of yet, to show any effect in the fish. However, if these levels continue to rise, it will be a large issue as many people have fish as a large part of their diet. Both of these compounds have metabolites which exist in anionic forms. Sertraline undergoes de-amination and forms the

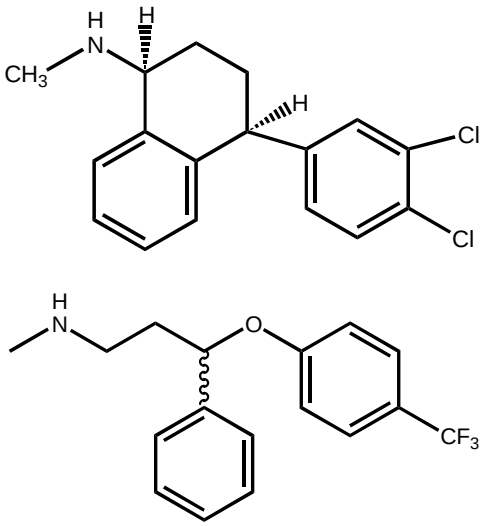

Figure 3. Chemical structures of sertraline (top, trade name Zoloft) and fluoxetine (bottom, trade name Prozac), two of the most popular antidepressant medicines to date.

sertraline ketone, which is often hydroxylated at the alpha carbon to form alphahydroxy sertraline ketone. Also, like propranolol, it is glucuronated. Fluoxetine forms both *p*-trifluoro-methylphenol and hippuric acid.

Detecting these drugs in the environment to understand their fate and transport is often very difficult. Due to the large variety of drugs, there is not a standard analytical method for detection[14]. Often a full analytical method must be developed for each drug, which is both time consuming and costly. Many people have turned to computer modeling to try to elucidate the compounds that will persist and/or bio-accumulate in the environment. The more persistence a compound exhibits, the more likely it will concentrate to levels closer to the therapeutic dose. By identifying the persistent compounds, researchers can focus their efforts on how to deal with these long lasting pollutants[14]. However, even after the pollutants of interest have been identified, analytical methods still need to be developed to accurately quantify their environmental concentrations.

Remediation

For remediation efforts, low cost and low energy methods are essential for large-scale industrial implementation. By developing highly stable materials, pollutant scrubbing could be accomplished at the source when the pollutant is still highly concentrated, as opposed to after dilution in the environment. This goal is far easier said than done. It

is not only a chemistry problem (hard to develop stable pollutant scrubbing materials), but also a business problem (adding industrial processes with very little chance of making money from the process).

Materials with exceptionally high surface area are ideal for pollutant scrubbing. The high surface area allows for a large number of binding sites. Extended 3-D porous materials (e.g. zeolites) generally have also a large internal surface area, making them ideal candidates. The rigidity of the network allows for size and shape exclusion resulting in selectivity. Layered 2-D materials (e.g. LDHs) are also used extensively for anion exchange. The lack of rigidity and possible expansion of the interlayer space in 2-D materials can allow for a wide variety of potential intercalators.

For most remediation efforts, affordability and reusability of the material are key. By reusing a material, the cost per use will decrease, making the remediation effort more economically feasible. However, there are cases when reusability is not desired. If the pollutant were exceptionally toxic (e.g. radioactive wastes), immobilizing the pollutant in a stable matrix would be desired[15]. Some examples of remediation materials will now be discussed.

Modified Resins

Organically modified resins are widely used as remediation tools due to the variety of chemical possibilities. These resins, often polystyrene or acrylic, may be designed to select for specific targets, but will always suffer from stability issues at high temperature or under harsh conditions. The resins for anion exchange often consist of quaternary amines bound to the styrene (Styrene-$NR_3^+X^-$, R = alkyl or aryl group, X = anion) packed in chromatography column. In a study performed on five commercially available resins, the pH range tested was 6.3 – 7.9[16]. While this is suitable for water treatment in dilute manners, these resins would most likely fail under harsher conditions in raw industrial wastewater. Due to the nature of the resin, separation from the exchange solution can be achieved at up to 99.9% efficiency, though uptake capacity remains the key issue for resins in terms of equivalents per gram.

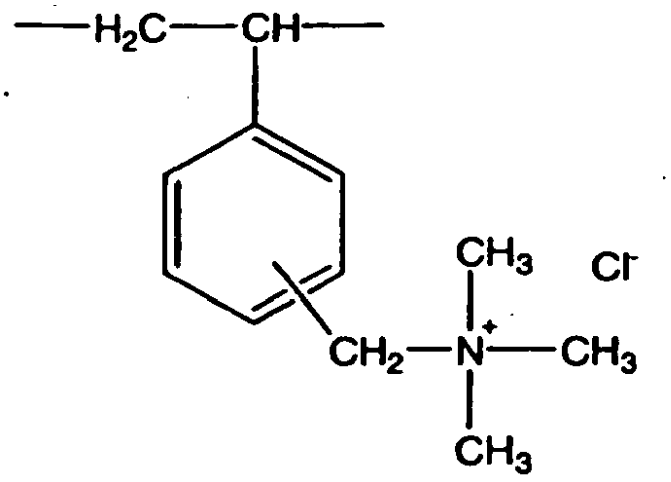

Figure 4. Basic chemical structure of polystyrene based anion exchange material. The ammonium group is charge balanced by an exchangeable anion.

The type of resin also changes the efficacy of the anion exchange. Acrylic resins have the ability to swell and exchange for more anions than styrene resins with the same degree of functional group loading[17]. The increased space allowed for by swelling will allow more access to the available functional groups. Styrene will not swell, and as anions are bound, they may sterically hinder the other available binding sites.

Layered Double Hydroxides

Layered double hydroxides (LDHs) follow the general formula of $[M^{2+}_{1-x}M^{3+}_{x}(OH)_2][A^{n-}_{x/n}\cdot mH_2O]$, where M^{2+} and M^{3+} are a range of metals (usually Mg^{2+} and Al^{3+}), x is the ratio of $M^{3+}/(M^{2+}+M^{3+})$, and A^{n-} are n-valent interlamellar anions (e.g. carbonate). These materials can be synthesized hydrothermally, at room temperature, or under reflux. LDHs, also known as hydrotalcites or anionic clays (Figure 5), can scrub water in two ways: anion exchange or reconstruction of the layers after calcination[18,19]. LDHs, generally, suffer from a lack of selectivity for pollutants of interest; both reconstruction and exchange favors the intercalation of carbonate anion (CO_3^-) over most other anions. Many efforts have been made to eliminate the affinity for carbonate by using a large variety of metals. Common M^{2+}/M^{3+} pairs include Ca/Al, Li/Al, Mg/Al, Ni/Al, Zn/Al, and Zn/Cr[20]. Both inorganic (e.g. halides, carbonate, sulfate) and organic (e.g. oxalate, dodecyl-sulfate) anions have been intercalated in the as synthesized materials.

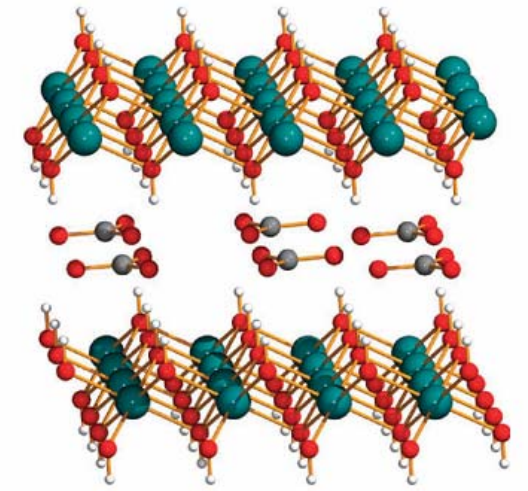

Figure 5. A cationic hydrotalcite with formula $Mg_6Al_2(OH)_{16}[CO_3^{2-}]$ [15]

LDHs have been investigated for use as a drug delivery vehicle. Researchers intercalated various pharmaceuticals to be released in a controlled manner. This shows that the interlayer space is capable of accommodating pharmaceuticals, such as diclofenac, naproxen, gemfrizobril, 4 – biphenylacetic acid, and others[21]. These materials were prepared *via* anion exchange after synthesis of the LDH with the formula $[LiAl_2(OH)_6]Cl{\cdot}H_2O$, which shows they do have the ability to enter the interlayer space despite their size. However, each of the anions was present in a 2x molar concentration over the LDH. In real world remediation settings, this will not be the case.

For remediation, room temperature anion exchange is preferred. High temperature calcination is energy intensive and will be a limiting factor in most remediation efforts utilizing LDHs. LDHs have great anion exchange capacity in batch

experiments, but are often limited by real world parameters, such as the presence of carbonate or other preferred intercalators (nitrate). Furthermore, removing the LDH from the anion exchange solution often requires time and energy consuming centrifugation.

Metal Organic Frameworks

Several groups have reported the synthesis and the host-guest chemistry of metal-organic frameworks (MOFs)[22,23]. They can be 1-D (chain), 2D (layered) or 3D. MOFs consist of metal centers or clusters joined by organic linkers. It is the large variety of organic linkers (Figure 6) that make MOFs attractive materials for pollutant trapping. These linkers can be designed with specific pollutants (or other applications) in mind. For example, groups have used 1,3,5 benzenetricarboxylic acid as a linker for the purpose of selectively trapping aromatic compounds through pi-pi interactions[15]. By altering the linker, the MOF can be rationally designed for intended use. Size and shape exclusion can be obtained by choosing various linkers that will alter the pore size, shape, and chemistry of the material.

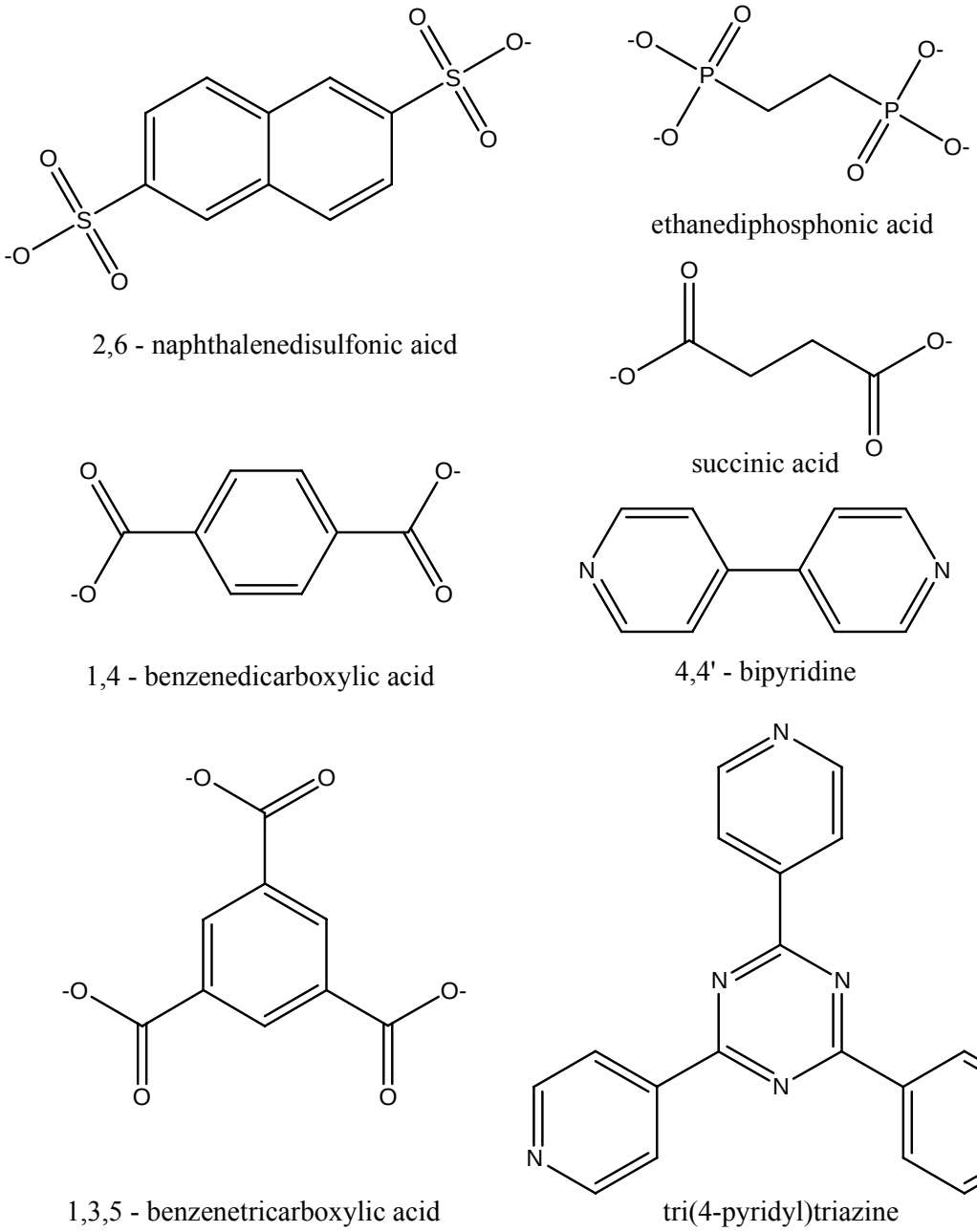

Figure 6. A sampling of some common organic linkers for MOFs. Includes carboxylates, sulphonates, phosphonates, and azole groups.

In terms of pollutant trapping, our group has recently reported two cationic-layered MOFs based on copper and silver[24]. These are layered materials that consist of metal

centers linked by 4,4-bipyridine. The positive charge exhibited by the layers is balanced by divalent ethanedisulfonate, with one oxygen atom from each sulfonate group interacting with a metal center. This weak interaction between the sulfonate and the metal center allows for anion exchange to take place with high yield. These materials were able to exchange for a variety of inorganic pollutants (e.g. perchlorate, nitrate), but were not shown to exchange for any organic anions.

While MOFs have ability to be designed for specific application by modification of the organic linker, they suffer from that very same moiety. The organic linker will always lead to a decrease in stability in comparison to its purely inorganic counterparts. It is always preferable to have extended inorganic connectivity such as metal oxide bonding in the host for much greater stability.

Layered Metal Hydroxides

Recently many cationic, layered metal hydroxides (LMHs) have been reported[25,26,27,28]. Like LDHs, these metal hydroxides are able to hold cationic charges due to the high degree of protonation in the layers. This decreases the negative charge contribution from the oxygen atoms. The layers are charge balanced by a wide variety of anions including nitrates, halides, sulfonates, and carboxylates. LMHs used for pollutant scrubbing will stay heterogeneous throughout the anion exchange allowing separation by simple vacuum filtration. This wide variety of anions, heterogeneity

throughout exchange, and their enhanced stability over MOFs and organically modified resins make them ideal candidates for remediation efforts.

Our group recently reported on a copper based LMH (Slug-26), which displays infinite M-O-M linkages in the layers balanced by divalent ethanedisulfonate (Fig. X). This was one of, if not, the first non LDH based cationic copper hydroxide. It exhibited both great thermal stability and a high anion exchange capacity for both metal pollutants and organic anions. Furthermore, the material remains heterogeneous throughout the exchange process, meaning separation can be achieved through simple vacuum filtration. Post exchange- characterization relies mainly on PXRD, FTIR, and TGA. It is not known how the organic or inorganic anions are intercalated due to lack of a quality single crystal for X-ray diffraction. This is due to the material losing some crystallinity during the exchange process. It is most likely that the anions intercalate in a variety of manners, not necessarily by a one to one substitution for the anion in the as synthesized material. By using variable chain length α,ω-dicarboxylates, a clear trend can usually be seen in the relationship between chain length and interlayer distance. Interlayer distance will, generally, increase linearly with an increase in the number of methylene units in the dicarboxylate. However, anions do have the possibility to intercalate at various angles or even parallel to the cationic layers, which will cause deviation from the linear relationship.

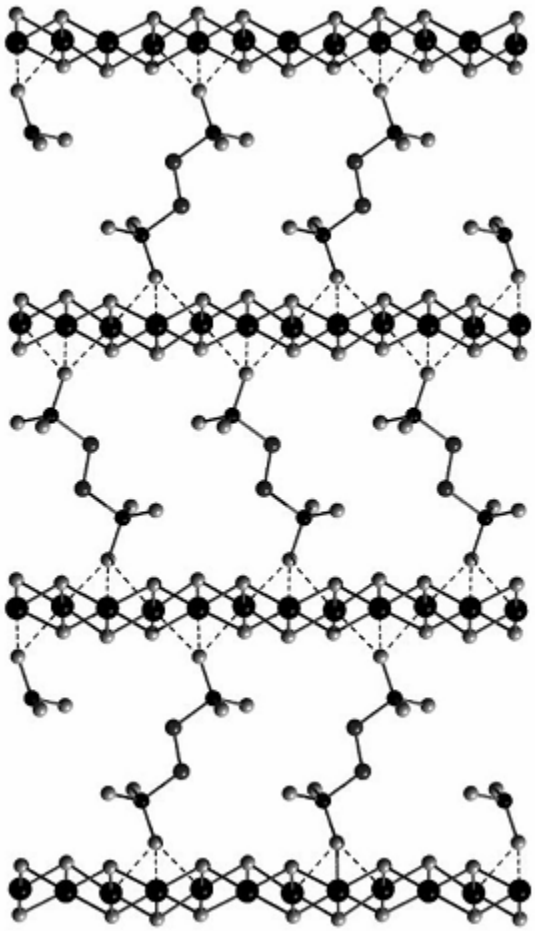

Figure 7. Interlayer view of Slug – 26. Infinite layers of $Cu_4(OH)_6$ balanced by divalent ethanedisulfonates.

A large variety of lanthanide based LMHs have been published recently[20,22]. Whole classes of hydroxynitrates (with the general formula $Ln_2(OH)_5NO_3{\cdot}H_2O$ (Ln = Y, Eu-Er)) and hydroxyhalides (with the general formula $Ln_2(OH)_5X{\cdot}1.5H_2O$ (X = Cl, Br; Ln = Y, Dy, Er, Yb)) synthesized hydrothermally have shown to have excellent anion exchange capability with a wide variety of carboxylates ($-COO^-$) and sulfonates ($-SO_3^-$) including phthalate, terephthalate, succinate, maleate, malonate, and anthraquinonedisulfonate, to name a few. One of the issues with these materials is the anion being released upon exchange. The release of nitrate or halides to an

aqueous environment is not ideal. Halogenation of dissolved organics can lead to harmful effects in aquatic and terrestrial life. Nitrate pollution has long been studied due to its prominence in the agriculture industry.

LMHs offer the ability to be coupled directly to industrial processes. With robust chemical and thermal stability, raw industrial wastes could be treated on site. This would offer several advantages opposed to treating downstream; the pollutant of interest will be at a high concentration, which may help overcome selectivity issues of the materials used to trap. To fully couple these remediate materials to an industrial process, the synthesis will need to be scaled up significantly. Scaling up reactions is not with out difficulty; however, some LMHs can be synthesized at room temperature. Precipitation synthesis at room temperature requires very little energy input, which is ideal for a remediation application.

Experimental

Synthesis: erbium (III) chloride hydrate (1.22g, $ErCl_3 \cdot xH_2O$, Alfa Aesar, 99.9%), 1,2-ethanedisulfonate disodium salt (0.22g, $NaO_3SCH_2CH_2SO_3Na$, Acros Organics, 99%), triethylamine (0.424g, Aldrich, 99%) and deionized water (10 g) were weighed into a 15 mL autoclave. The autoclave was sealed and heated statically at either 175 °C for 5 days or 200 °C for 2 days under autogenous pressure. The autoclaves were

allowed to cool in a fumehood. Pink needle-like crystals were obtained *via* vacuum filtration and rinsed with DI water. Products were examined by IR, PXRD, and TGA.

Exchange: Slug-27 was set to exchange with molar excess amounts of anions in aqueous solution. α,ω-alkanedicarboxylates of various chain lengths (malonic acid, succinic acid, glutaric acid, and adipic acid) were used to investigate the effect of chain length on interlayer distance. Aromatic dicarboxylates (p-terephthalic acid, 2,6-naphthalenedicarboxylic acid) were also studied in regards to intercalation chemistry. The reaction mixture was stirred for 24 hrs. Solids were obtained *via* vacuum filtration and rinsed with DI water. Solids were examined by IR, PXRD, and TGA.

IR: FTIR spectroscopy of synthesized and exchanged materials was performed using KBr pellets on a Perkin Elmer Spectrum One FTIR. Scans were run from 4000 to 450 cm^{-1} with a resolution of 4 cm^{-1}.

SCXRD: Data was collected on a Bruker APEX II CCD area detector X-ray diffractometer using graphite monochromated Mo-Kα radiation (λ = 0.71073 Å). Structure was solved using direct methods using SHELX.

PXRD: Spectra were obtained on two instruments: 1) Rigaku Miniflex II Plus scanned samples with Cu-Kα radiation (λ = 1.5418 Å) from 2˚to 40˚ 2-theta, at a rate of 2˚/min, and a step width of 0.02˚; 2) Rigaku Smartlab X-ray Diffractometer was used

for high temperature *in-situ* scans. The various temperature points were chosen based on the TGA traces of the materials. Each sample was scanned with Cu-Kα radiation (λ = 1.5406 Å) from 2˚to 40˚ 2-theta at a rate of 3˚/min, and a step width of 0.02˚.

TGA: Thermogravimetric Analysis was performed on a TA Thermoanalyzer 2050. Samples were heated in an aluminum pan with a Pt wire at a rate of 10˚C/min.

Results and Discussion

Synthesis and Structure

$Er_{12}(OH)_{29}(H_2O)_5(O_3SCH_2CH_2SO_3)_{3.5}\cdot 4H_2O$ (Slug-27) forms at 200 ˚C under hydrothermal conditions. The material crystallizes biphasically with needle like crystals interspersed among fibrous crystalline material. The morphology is best described as cotton candy-like. The average yield is 39.9 % based off a theoretical yield of 0.885 grams, with the erbium chloride reagent being the limiting reagent.

The overall structure of Slug-27 (solved by single crystal XRD) consists of cationic corrugated erbium hydroxide layers balanced by interlamellar ethanedisulfonic acid (EDS) anions. Slug-27 exhibits very low symmetry, with 12 crystallographically independent erbium centers (Fig. 1) and 4 different modes of EDS intercalation (Fig. 2, Fig. 3). Nine of the erbium centers are 8 coordinate, while the other three are 7 coordinate. One of the four EDS molecules “floats” in the interlamellar space and is stabilized by hydrogen bonding to crystallographic water and hydroxide groups on

the inorganic layers. Two of the four EDS molecules are singly bound to the layer and have the free sulfonate group stabilized by the same type of H-bonds. The last EDS bridges the interlamellar space and is crystallographically symmetric around its C-C bond, thus the formula has 3.5 EDS molecules instead of 4.

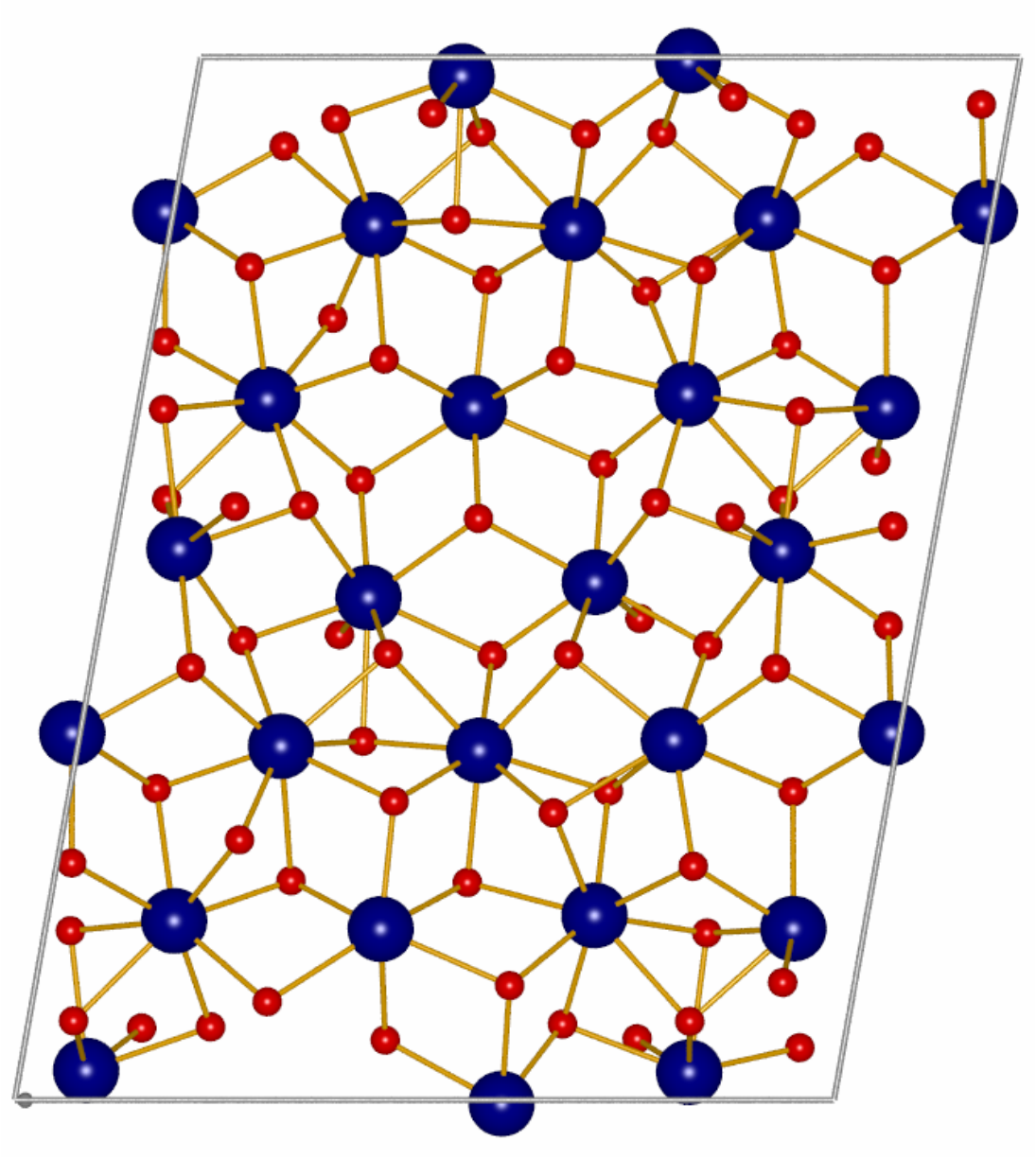

Figure 8. Crystallographic view of $Er_{12}(OH)_{29}(H_2O)_5$ layer of Slug-27 along the crystallographic b-axis (Er blue, O red). Hydrogen atoms omitted for clarity.

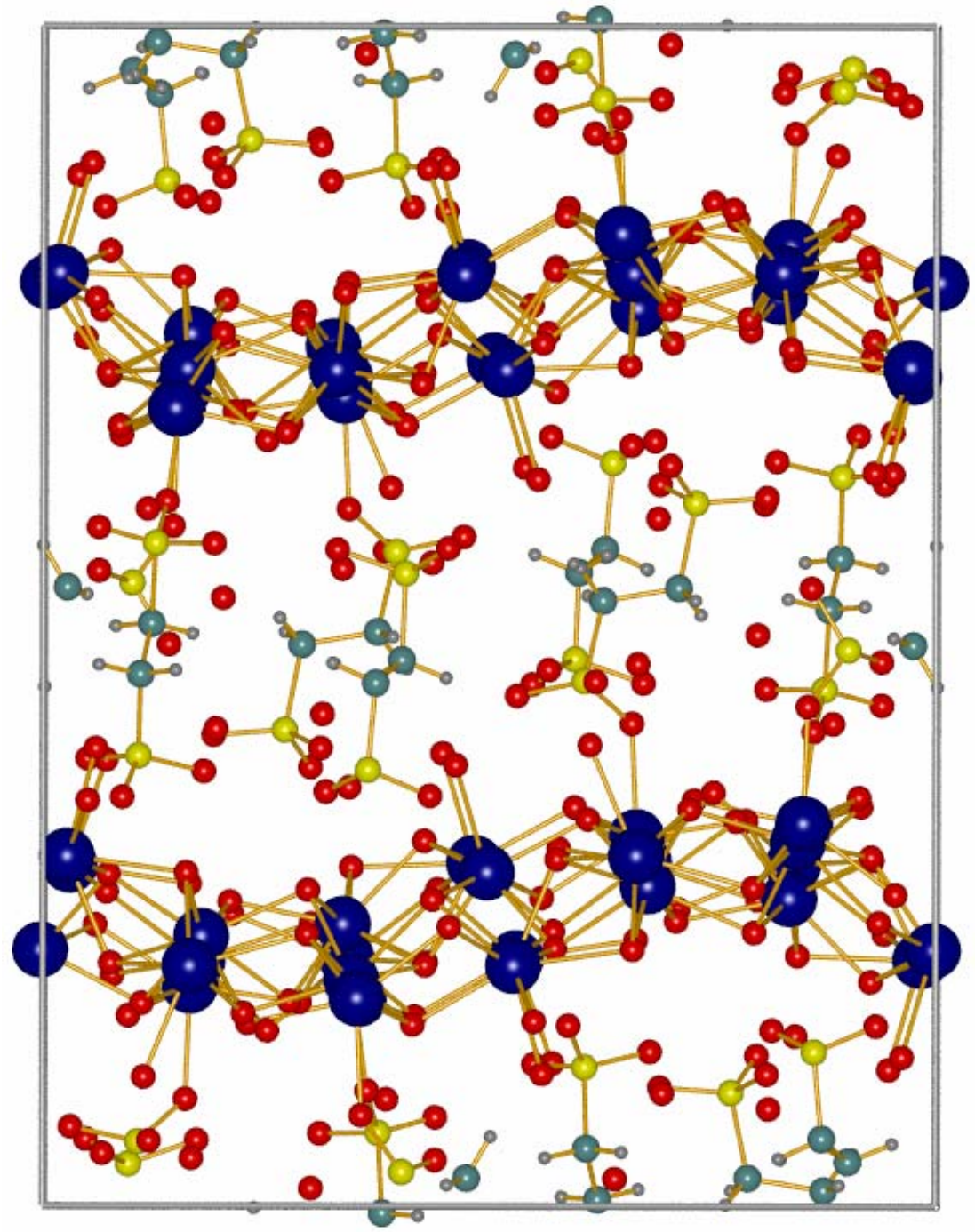

Figure 9. Crystallographic view of the interlayer EDS of Slug-27 along the crystallographic a-axis (Er blue, O red, S yellow, C teal). Layer hydrogens omitted for clarity. For better clarity of EDS, see Figure 3.

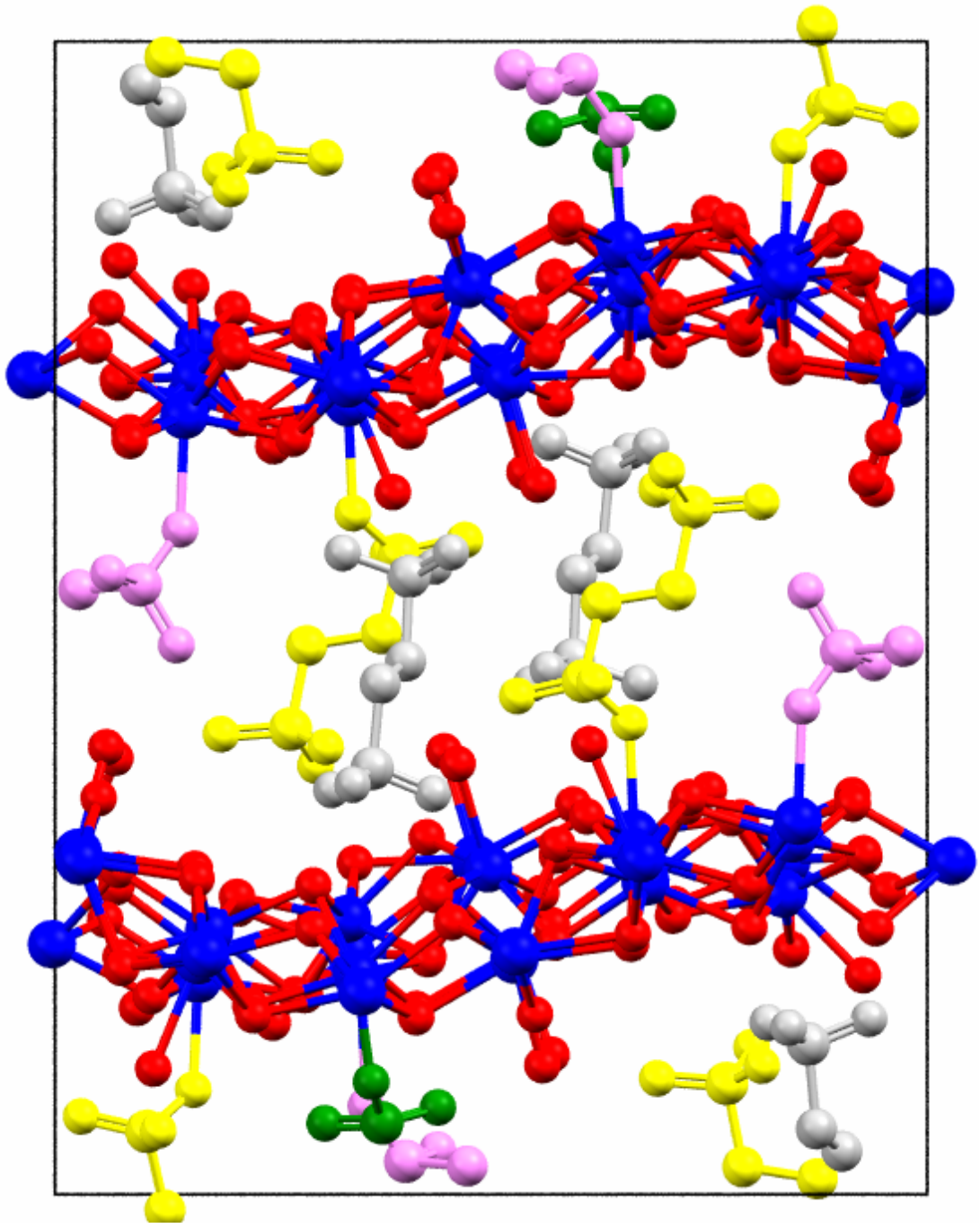

Figure 10. Alternate view of the interlayer space with each EDS colored individually for clarity (white – floating; yellow and green – singly bound; pink – bridging and crystallographically symmetric about the C-C bond). Hydrogens omitted for clarity.

In comparison to Slug-26 (Figure 7), Slug-27 may have the potential for better anion exchange properties. The EDS in Slug-26 has both sulfonate groups bound to the layers. In Slug-27, with 4 modes of EDS intercalation (Figure 10), only one of the modes has both sulfonate groups bound to the layers. Two of the modes of EDS intercalation are bound through one sulfonate group while the other is balanced through hydrogen bonding. The last mode of EDS intercalation has no interaction with the layer other than through hydrogen bonding and electrostatic interaction. With fewer interactions between the layer and the intercalating anion, greater anion exchange may be achieved. The exchange properties of the material will need to be investigated in depth with a variety of intercalates.

The PXRD spectra of Slug-27 (Figure 11) is dominated by the intense (001) reflection of the erbium in the cationic layers. The principle (001) peak is at 7.60˚ (2θ) and the higher order reflections appear at 15.2˚ and 22.8˚. When comparing the projected PXRD from the single crystal data to experimental PXRD, the principle peak is shifted to slightly higher angle in the experimental pattern. This shift is likely due to the preferential packing of the layers as the material is ground in preparation for analysis. Using Bragg's law ($d = n\lambda/2\sin\theta$) the interlayer distance was calculated from the 7.60˚ peak to be 11.5 Å. Few other intense peaks appear due to the relative disorder of the interlayer space and high diffracting capability of the erbium centers.

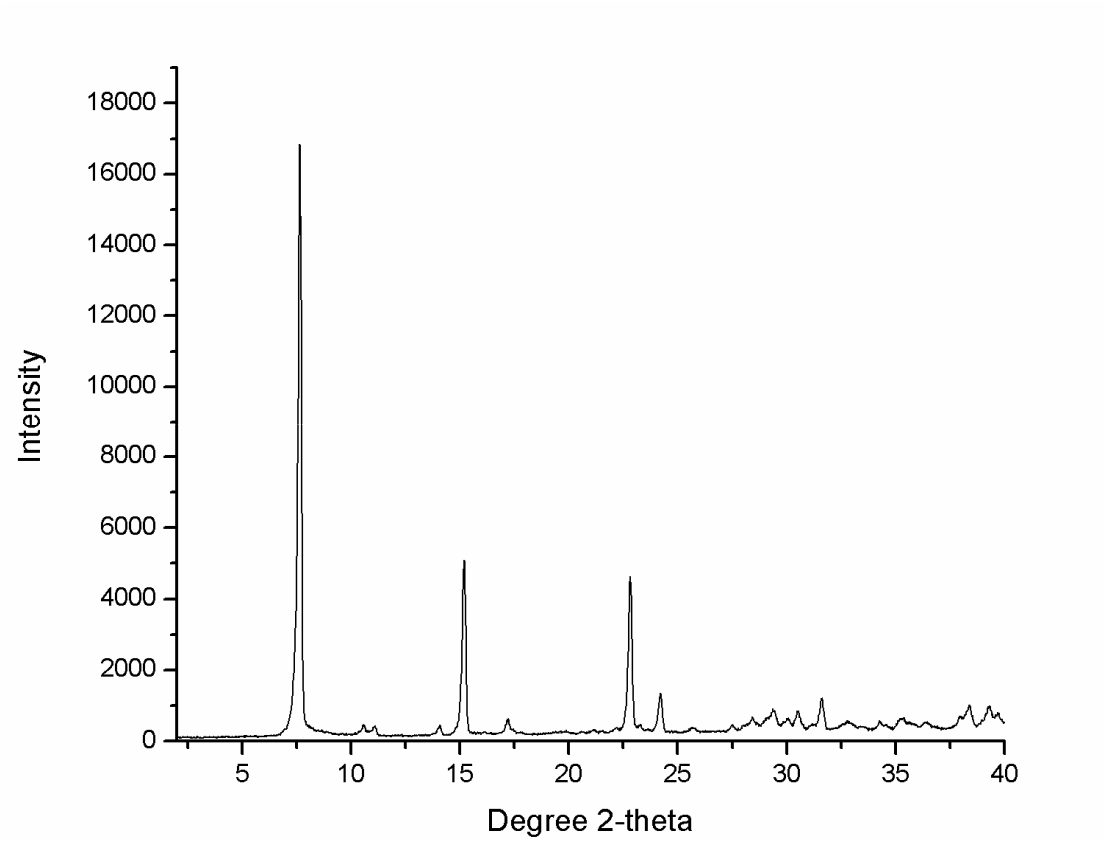

Figure 11. PXRD spectra of Slug-27. Principle peak at 7.60˚, with higher order (00l) reflections observed at 15.2˚ and 22.8˚.

The intercalation chemistry was investigated using a variety α,ω-dicarboxylates and the products analyzed by FTIR and PXRD. Often the chain length of the intercalating anion can be directly correlated to the interlayer distance by plotting d (from the Bragg equation) *vs*. methylene units. From PXRD spectra of the exchanged materials (Figure 12), the interlayer distances did not shift as expected with increasing chain length of the dicarboxylates (Malonic < Succinic < Glutaric < Adipic, Table 1).

Table 1. 2-theta and d-spacing values for Slug-27 and exchanged materials

Anion	2-Theta (°)	d-spacing (Å)
As-synthesized	7.6	11.5
Malonate	8.9	9.9
Succinate	9.4	8.8
Glutarate	7.8	11.4
Adipate	6.1	14.6

The as synthesized material has a principle peak at 7.60 degrees 2-theta, giving an interlayer distance of 11.5 Å. It would be expected that the adipate [$^{-}O_2C(CH2)_4CO2^{-}$] and glutarate[$^{-}O_2C(CH2)_3CO2^{-}$] would shift the principle (001) peak to lower 2-theta values as the interlayer distance would increase, and that succinate[$^{-}O_2C(CH2)_2CO2^{-}$] and malonate [$^{-}O_2CCH_2CO_2^{-}$] would shift the peak to higher 2-theta values as interlayer distances got smaller. Glutarate shifted the principle (001) peak very little, but the appearance of carboxylate peaks in the IR spectrum (Figure 13) indicates exchange has taken place. Unexpectedly, the succinate shifted the principle (001) peak to higher 2-theta values than malonate. This indicates that the interlayer distances in the succinate exchanged materials are smaller than that of malonate despite the fact that succinate has a longer chain length. This is most likely due to preferred crystal packing with succinate intercalating at a more parallel angle to the layers. Adipate shifted the principle peak to the lowest angle of the carboxylates as expected.

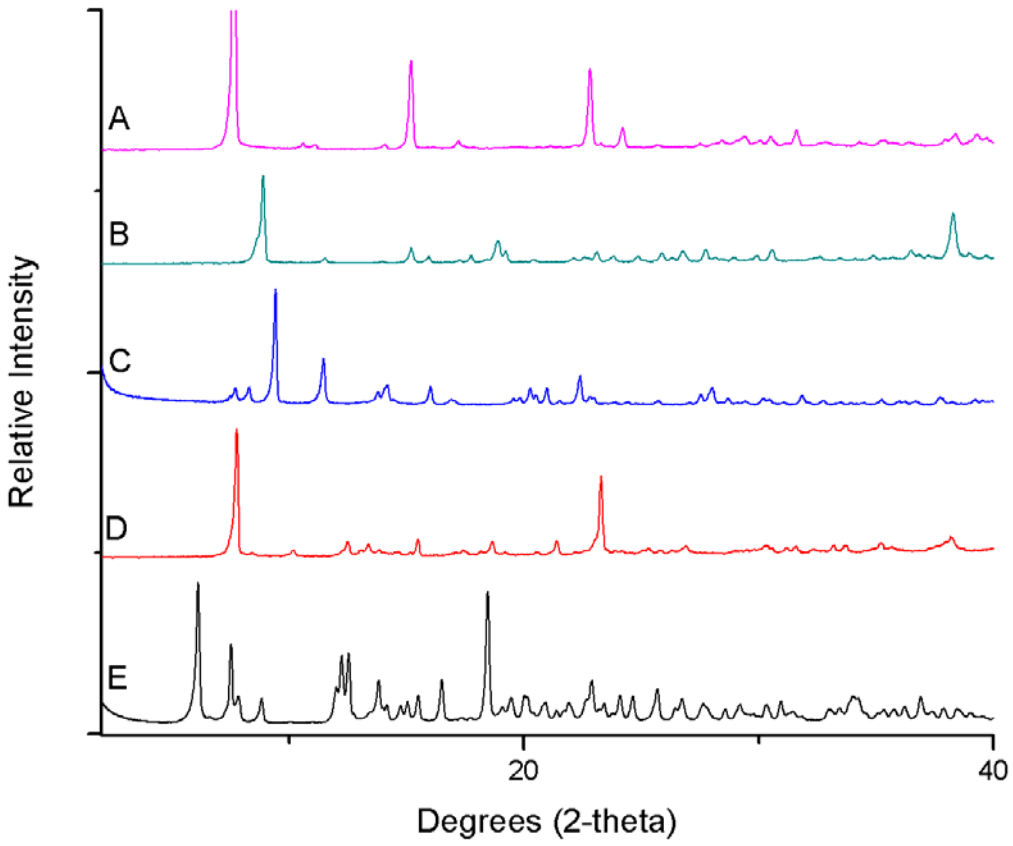

Figure 12. PXRD of SLUG-27: (A) as-synthesized [$^{-}O_3SCH_2CH_2SO_3^{-}$]; (B) exchanged with malonate [$^{-}O_2CCH_2CO_2^{-}$]; (C) exchanged with succinate [$^{-}O_2C(CH_2)_2CO_2^{-}$]; (D) exchanged with glutarate [$^{-}O_2C(CH_2)_3CO_2^{-}$]; (E) exchanged with adipate [$^{-}O_2C(CH_2)_4CO_2^{-}$].

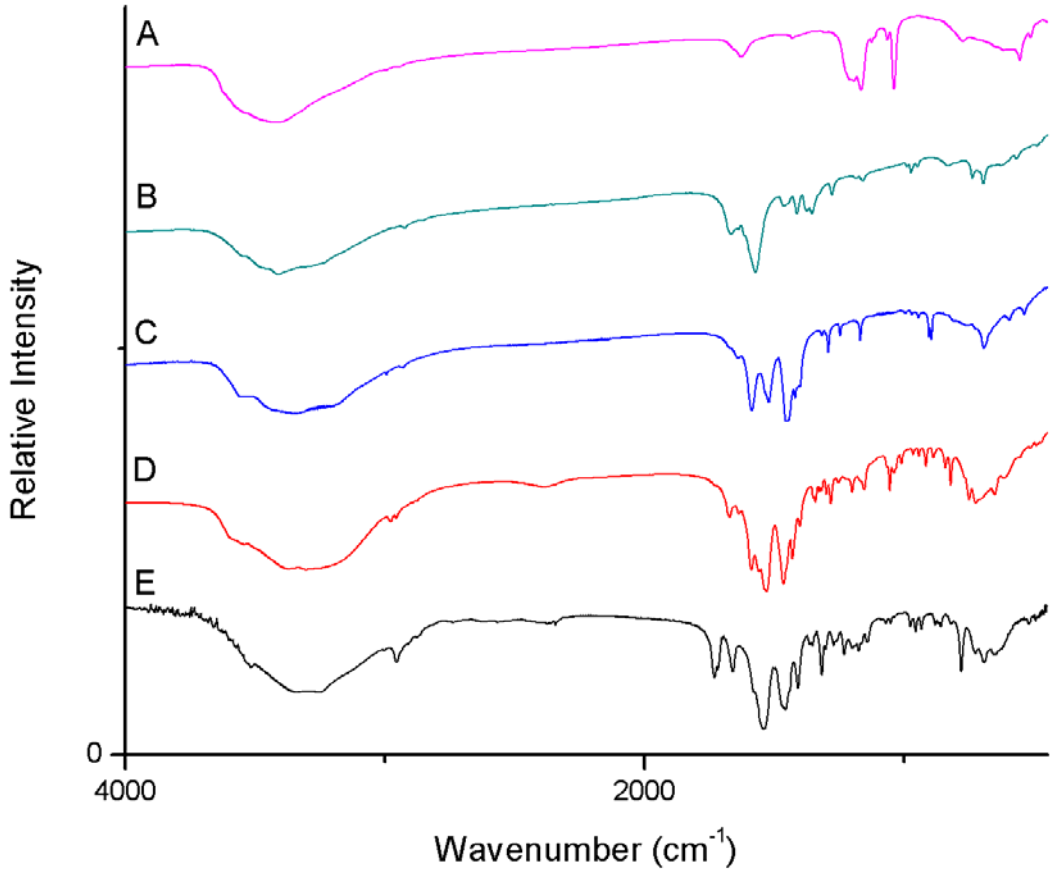

Figure 13. FTIR spectra of Slug-27: (A) as-synthesized [$^{-}O_3SCH_2CH_2SO_3^{-}$]; (B) exchanged with malonate [$^{-}O_2CCH_2CO_2^{-}$]; (C) exchanged with succinate [$^{-}O_2C(CH_2)_2CO_2^{-}$]; (D) exchanged with glutarate [$^{-}O_2C(CH_2)_3CO_2^{-}$]; (E) exchanged with adipate [$^{-}O_2C(CH_2)_4CO_2^{-}$].

Variable temperature *in-situ* PXRD (Figure 14) shows the thermally induced transitions of the material as it is heated from room temperature to 1000 ˚C. Slug-27 is quasi-stable to ~300 ˚C as water is driven out of the interlamellar space. The visible peak broadening and loss of intensity indicates reduction in crystallinity as the hydrogen bonding networks that stabilize the sulfonate groups are likely lost. The principle peak shifts to higher 2-theta values indicating reduction in layer-to-layer distance. As temperatures increase further (> 300˚C to < 700 ˚C), a fully amorphous

material is observed with no sharp peaks. Above 700 °C, new peaks begin to form at 27 to 33 degrees 2-theta, which are indicative of erbium sulfide (28.56° and 33.09°, ICCD 53-414). Above 900 °C, the material begins to shift towards erbium oxide (29.28° and 33.94°, ICCD 94-888) as the sulfur is driven out.

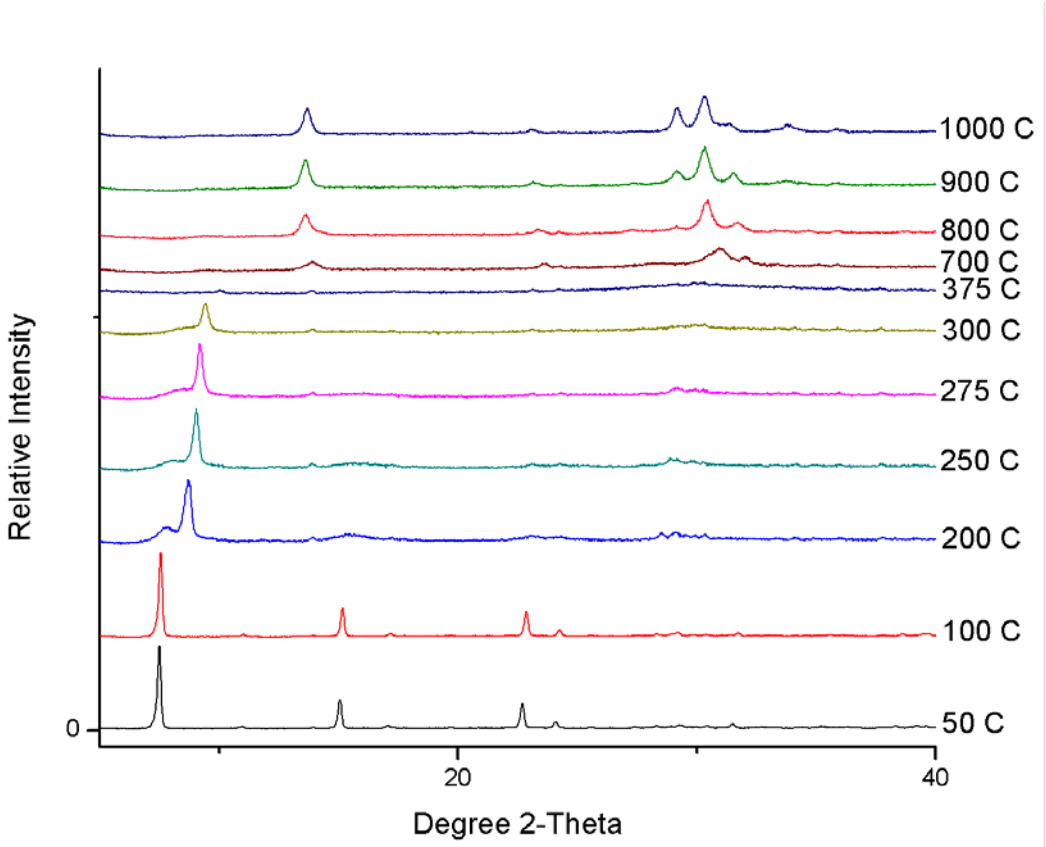

Figure 14. Variable temperature *in-situ* PXRD of Slug-27. Scans at 400, 425, 500, and 600 ˚C were identical to the amorphous scan at 375 ˚C and are omitted for clarity.

Variable temperature in-situ PXRD of the exchanged materials yielded very similar spectra to the as-synthesized material (Figure 15). The same quasi-crystalline character was observed up to 450 ˚C before becoming completely amorphous from > 450 ˚C to 550 ˚C. This transition can also be seen in the TGA trace of the succinate

exchanged material (Figure 16). At 450 ˚C there is a significant loss of mass as seen in the TGA scan, which correlates to the loss of crystallinity as seen in the VT-PXRD at the same temperature. A t 600 ˚C erbium oxide begins to form, as opposed to the formation of a mixed sulphide/oxide in the as synthesized material. As the temperature increases to 1000 ˚C, the erbium oxide peaks begin to sharpen as the material becomes more crystalline. This is further confirmation of the complete and clean exchange of dicarboxylates for the EDS. If the exchange had not gone to completion, remnants of the sulfonate groups would have lead to the formation of a mixed sulphide/oxide.

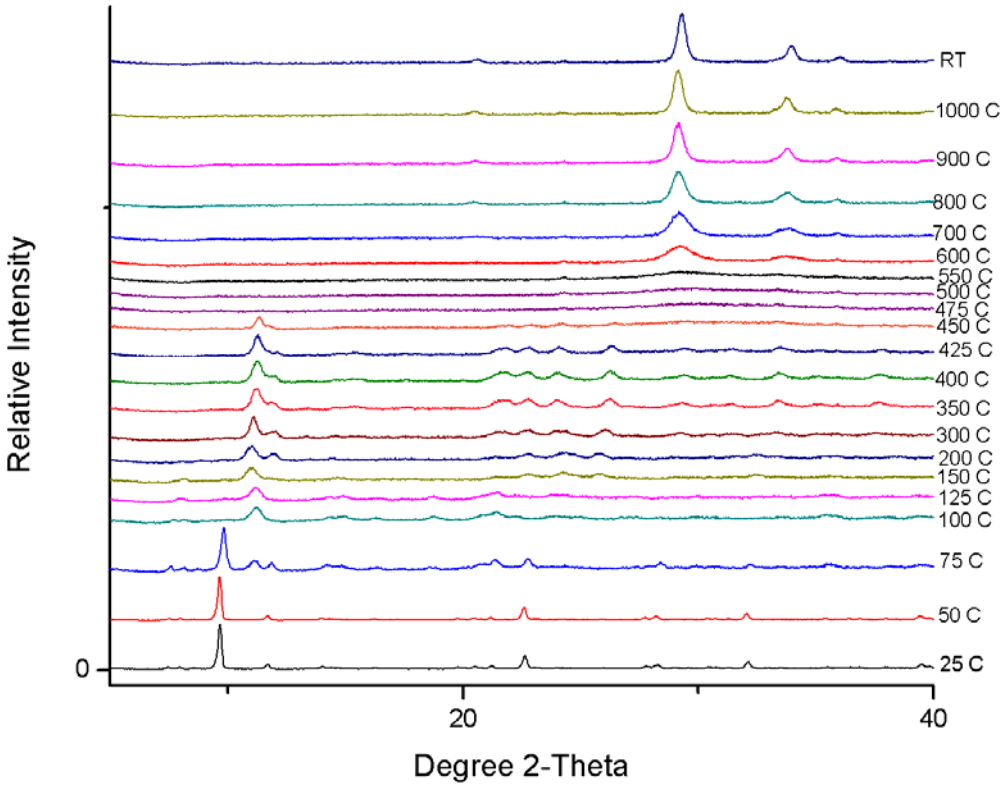

Figure 15. VT-PXRD for the succinate [$^{-}O_2C(CH_2)_2CO_2^{-}$] intercalated materials. Formation of erbium oxide starting at 600˚ C at 30˚ 2-theta confirms no sulfonate remained after exchange.

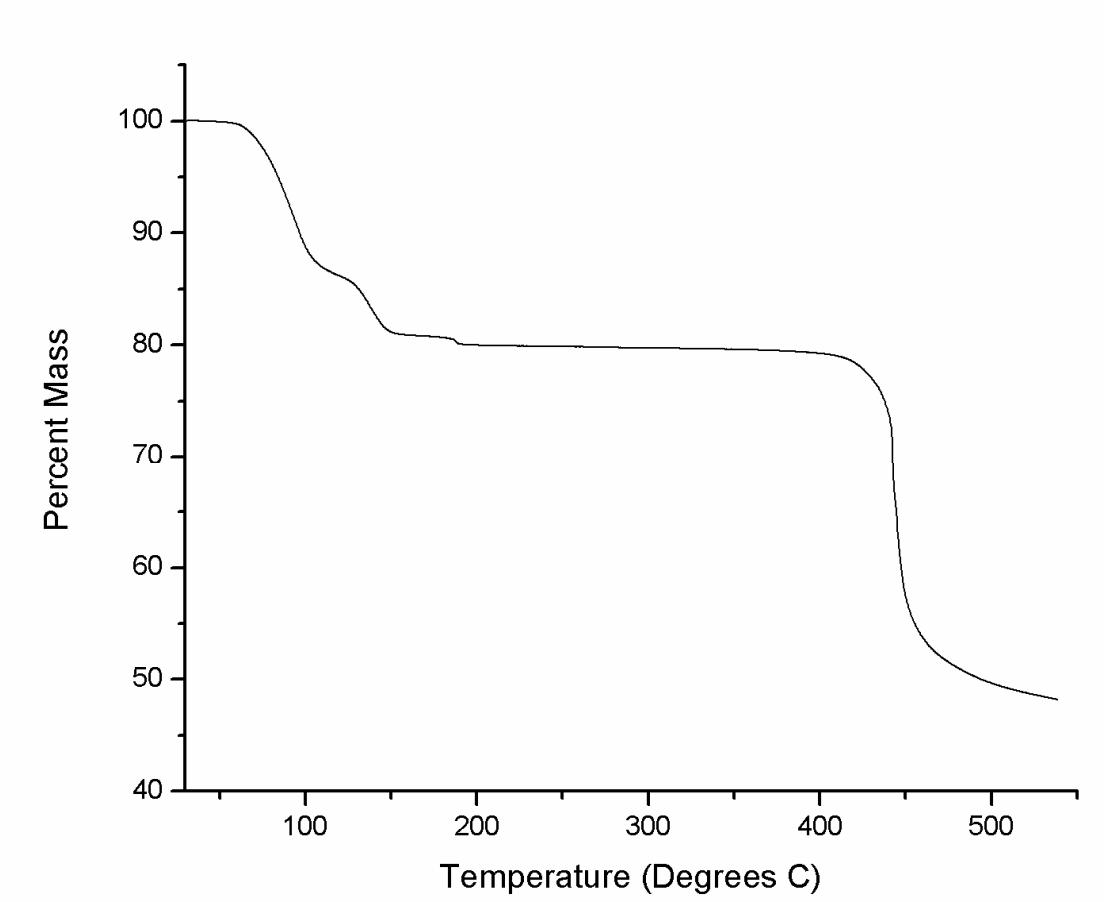

Figure 16. TGA trace of Slug-27 exchanged with succinate. Heating was at 10 ˚C/min from 30 ˚C to 550˚C.

In order to better investigate the transitions occurring, another *in-situ* VT-PXRD experiment was run with a scan at every 10 ˚C between 100 – 200 ˚C (Figure 17). The loss of water led to loss of intensity and peak broadening as expected. Unexpectedly, after cooling and sitting for 24 hours, the sample fully rehydrated and yielded the same spectrum as before heating. This rehydration event was studied further by TGA (Figure 18). TGA showed the material could regain most of its lost mass very quickly (to within 0.6% and 0.78% of the original mass for the second and third trials,

respectively). Repeated trials on the TGA (one hour between runs to allow for cooling) show the same mass loss profile as the first run, meaning that the material is able to rehydrate fairly quickly and is not structurally altered. PXRD of the material taken every 15 minutes after TGA to 200 ˚C showed the process to fully regain crystallinity requires at least 4 hours.

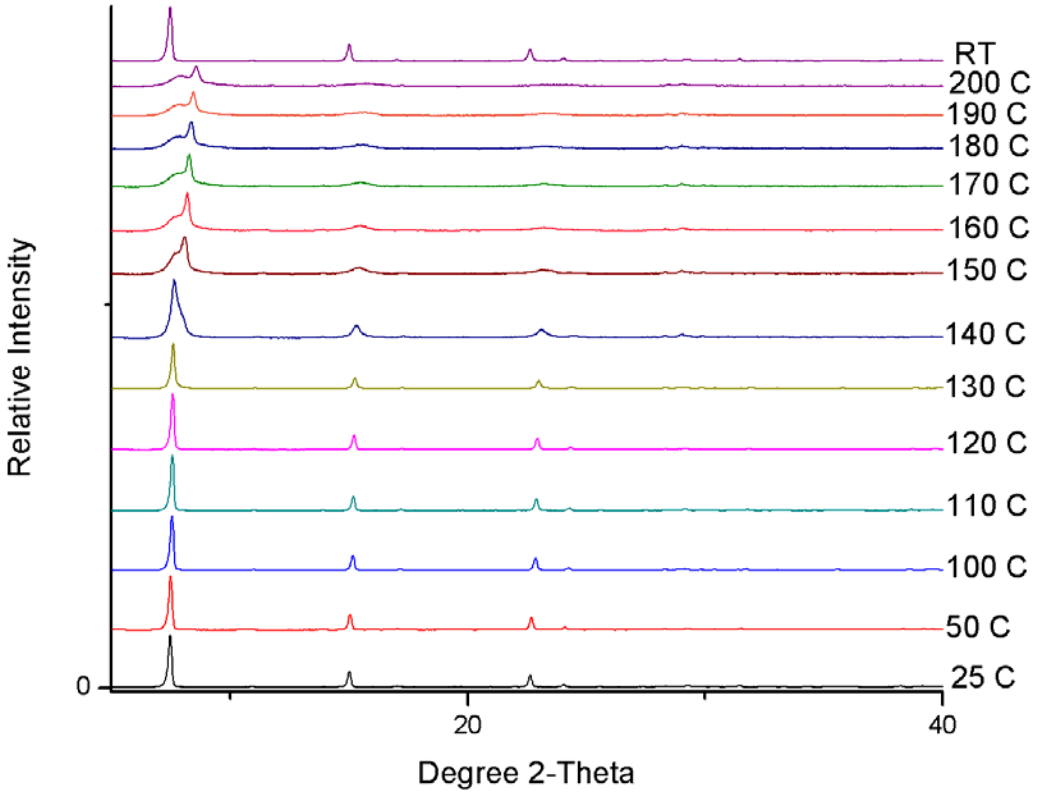

Figure 17. *in-situ* VT-PXRD up to 200˚ C to observe the dehydration and subsequent rehydration after cooling.

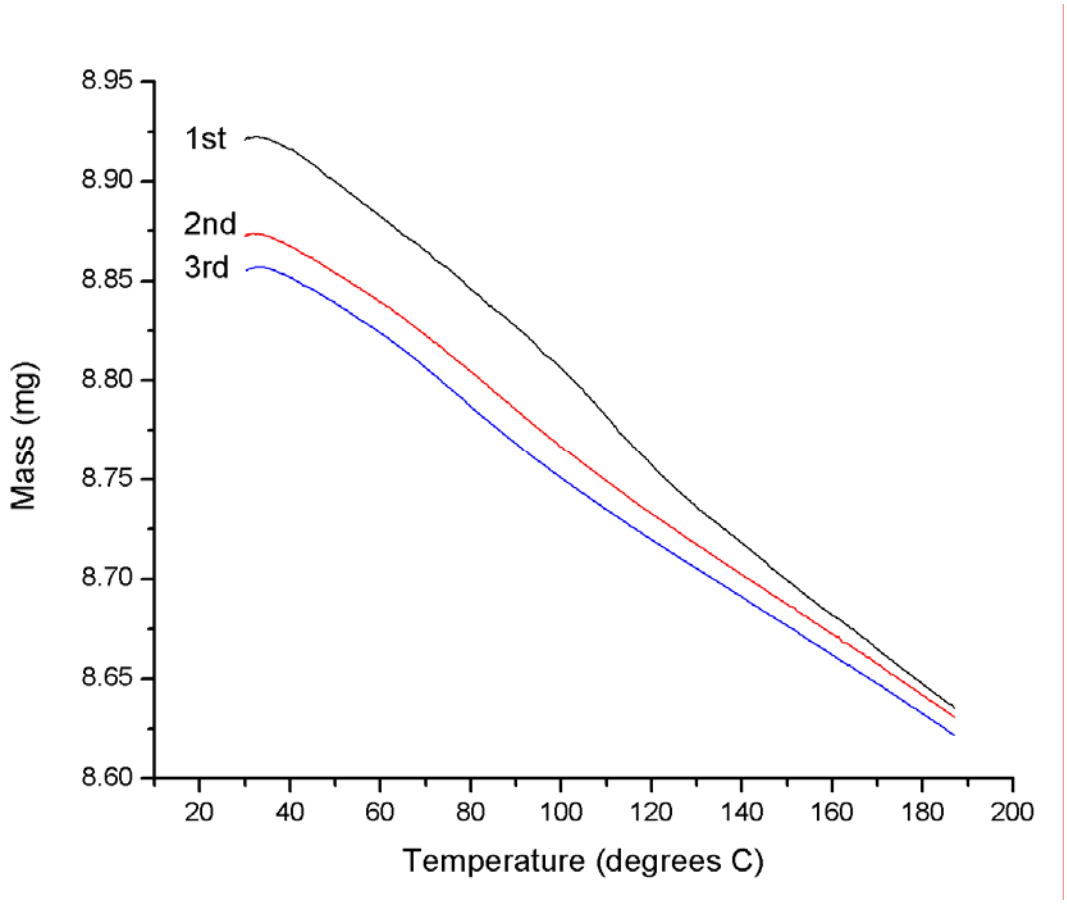

Figure 18. TGA trace of Slug-27 for rehydration studies.

The first TGA run showed a 3.42% mass loss (Table 2). If the 4 crystallographic waters were removed, there would be a mass loss of 2.16%. If all water were to be removed (4 crystallographic, 5 bound to the layers, equals 9 total waters) there would be a 4.8% mass loss. The 3.4% mass loss is right in the middle of these two values. This is not concerning because by analysis of the VT-PXRD of Slug-27 (Figure 13) shows that water loss most likely continues at temperatures up to ~275 ˚C. The two subsequent TGA trials showed a mass loss of 2.89% and 2.80% for the second and third trial, respectively. Lower percentages of mass loss are expected for the

subsequent trials due to incomplete rehydration of the material in the time between the trials.

Table 2. TGA masses and percent mass loss

Trial	1	2	3
Starting mass (mg)	8.941	8.887	8.871
Finished mass (mg)	8.635	8.631	8.621
Mass loss (%)	3.42%	2.88%	2.82%

Conclusions and Future Work

Slug-27 is another example of an LMH that could lead to the way to better industrial pollutant scrubbing materials. While it is very important to develop remediatory materials for the pollutants that are currently in and continually being introduced to the environment, it would be more beneficial to attempt to stop the pollutants from ever entering the environment. Obviously, this is no easy task. Due to our capitalist society, very few, if any, businesses will voluntarily invest money into a project that will garner them little profit. One could argue that the public opinion could sway some companies, but first the public must have an opinion on the issue. Of course, the vast majority of people will most likely say that pollution is bad. However, if we are talking about chemical pollutants at ng/L to μg/L concentrations, then it is far too abstract for most people. To the person not involved in a scientific field, what does a part per billion actually mean?

Slug-27 offers a myriad of possible applications beyond pollutant trapping. One group has previously used a 3D MOF to desiccate various organic solvents, including benzene, THF, acetone, and ethanol among others[29]. The material shows the same powder pattern before being dehydrating to act as a dessicant and after re-hydration meaning the material retains its original structure. We have seen the same for Slug-27 after VT-PXRD to 200˚ C (Figure 15); the material retained its original structure after rehydration.

It would also be beneficial to look at the effect of dehydration has on the exchange capabilities of the material. It was shown that the erbium hydroxide layers remained stable up to ~250˚ C, at which temperature the interlayer space lost order due to lack of stabilizing water. This destabilization of the interlayer space may change the selectivity of the intercalation properties of Slug-27, which could open the door to a larger variety of pollutants. The pre-heating would be analogous to the calcination used for LDHs. As of yet, no oxo-anions (perchlorate, perrhenate, permanganate) have been successfully exchanged for by Slug-27. These pollutants are targets of great interest due to their high aqueous solubility and effect on human life. Perchlorate (an inhibitor of iodine uptake in the thyroid) has been found in drinking water all over the southwestern United States, mainly as a result of rocket testing at various test sites.

It is also of utmost importance that whatever anion is being released upon uptake of pollutants is not a pollutant itself. The EDS used in our materials is not an environmentally friendly anion. Therefore, it is important to either pre-treat the material to ensure a benign anion is released, or to capture the EDS after exchange. Pre-treatment would be preferred because of the control that can be exhibited over the process. The EDS can be isolated easier from a controlled pre-treatment than after exchange in an aqueous solution with a large variety of components. The reclaimed EDS could then be used as precursor for another batch of Slug-27 (or other material) synthesis.

Reusability of Slug-27 should also be further investigated. To date, no subsequent exchange has taken place after the first exchange process. The pollutant would need to removed and replaced with another anion to balance the layers. Again, it is important that the anion used to remove the pollutant from the layers is not a pollutant itself. If dehydration of the material, as discussed earlier, affects the exchange properties, it may be exploited to open the path to reusability

References

[1] Daughton, C.G., Ternes, T.A. *Pharmaceuticals and Personal Care Products in the Environment: Agents of Subtle Change?* Environmental Health Perpspectives Special Report. **1999**. Volume 107, supplement 6.

[2] Benotti, M.J, Trenholm, R.A, et al. *Pharmaceuticals and Endocrine Disrupting Compounds in U.S. Drinking Water.* Environ. Sci. Technol. **2009**, 43, 567-603.

[3] Kümmerer, Klaus. *Drugs in the environment: emission of drugs, diagnostic aids and disinfectants into wastewater by hospitals in relation to other sources – a review.* Chemosphere. **2001**, 45, 957-969.

[4] Fent, K. Weston, A.A, Caminada, D. *Ecotoxicology of human pharmaceuticals*. Aquatic Toxicology. **2006**, 76, 122-159.

[5] Kime, D.E. *A strategy for assessing the effects of xenobiotics on fish reproduction.* The Science of the Total Environment. **1999**, 225, 3 – 11.

[6] Whitehorn, P.R., O'Connor, S., Wackers, F.L., Goulson, D. *Neonicotinoid Pesticide Reduces Bumble Bee Colony Growth and Queen Production*. Science, **2012**. 336, 351 – 352.

[7] Antonić, J. Heath, E. *Determination of NSAIDs in river sediment samples.* Anal. Bioanal. Chem. **2007**, 381, 1337-1342.

[8] Gentili, A. *Determination of non-steroidal anti-inflammatory drugs in environmental samples by chromatographic and electrophoretic techniques.* Anal. Bioanal. Chem. **2007**, 387, 1185-1202.

[9] Schwaiger, J., Ferling, H., Mallow, U., Wintermayr, H., Negele, R.D. *Toxic effects of the non-steroidal anti-inflammatory drug diclofenac. Part I. Histopathological alterations and bioaccumu- lation in rainbow trout.* Aquat. Toxicol. **2004,** 68, 141–150.

[10] Huggett, D.B., Brooks, B.W., Peterson, B., Foran, C.M., Schlenk, D., *Toxicity of selected beta adrenergic receptor-blocking pharmaceuticals (B-blockers) on aquatic organisms.* Arch. Env- iron. Contam. Toxicol. **2002,** 43, 229–235.

[11] Lee, H-B., Peart, T.E., Svoboda, M.L., Backus, S. *Occurrence and fate of rosuvastatin, rosuvastatin lactone, and atorvastatin in Canadian sewage and surface water samples.* Chemosphere. **2009**. 77, 1285 – 1291.

[12] Stancu, C., Sima, A. *Statins: Mechanism of action and effects*. Journal of Cellular and Molecular Medicin. **2001**. 5, 378 – 387.

[13] Bellosta, S., Paoletti, R., Corsini, A. *Focous on Clinical Pharmacokinetics and Drug Interactions.* Circulation. **2004**. 109, III-50 – III-57.

[14] Howard, P.H., Muir, D.C.G., *Identifying New Persistent and Bioaccumulative Organics Among Chemical Commerce II: Pharmaceuticals.* Environmental Science and Technology. **2007,** 45, 6938-6946.

[15] Oliver, S.R.J.. *Cationic inorganic materials for anionic pollutant trapping and catalysis.* Chem. Soc. Rev. **2009**. 38, 1868 – 1881.

[16] Humber, H., Gallard, H., Suty, H., Croue, J.P. *Performance of selected anion exchange resins for the treatment of a high DOC content surface water*. Water Research. **2005**, 39, 1699 -1708.

[17] Fu, P.L.K., Symons, J.M. *Removing Aquatic Organic Substances by Anion Exchange Resins*. American Water Works Association Journal**. 1990**. 82, 70-77.

[18] Burrueco, M.I., Mora, M., Jimenez-Sanchidrian, C., Ruiz, J.R. *Raman microspectroscopy of hydrotalcite-like compounds modified with sulphate and sulphonate organic anions.* J. Mol. Struct. **2013**, 1034, 38-42.

[19] Ulibarri, M.A., Pavlovic, I., Barriga, C., Hermosin, M.C., Cornejo, J. *Adsorption of anionic species on hydrotalcite-like compounds: effect of interlayer anion and crystallinity.* Applied Clay Science. **2001,** 18, 17-27.

[20] Khan, A.I., O'Hare, D. *Intercalation chemistry of layered double hydroxides: recent developments and applications.* Journal of Materials Chemistry. **2002**, 12, 3191 – 3198.

[21] Khan, A.I., Lei, L., Norquist, A.J., O'Hare, D. *Intercalation and controlled release of pharmaceutically active compounds from a layered double hydroxide.* Chemical Communications. **2001**. 2342 – 2343.

[22] Yaghi, O.M., Li, G., Li, H. *Selective binding and removal of guests in a microporous metal-organic framework*. Nature. **1995,** 378, 703-706.

[23] Li, H., Eddaoudi, M., O'Keeffe, M., Yaghi, O.M. *Design and synthesis of an exceptionally stable and highly porous metal-organic framework.* Nature. **1999**, 402, 276 – 279.

[24] Fei, H., Rogow, D.L., Oliver, S.R.J. *Reversible Anion Exchange and Catalytic Properties of Two Cationic Metal-Organic Frameworks Based on Cu(I) and Ag(I).* Journal of the American Chemical Society. **2010,** 132, 7202 – 7209.

[25] Fei, H., Oliver, S.R.J. *Copper Hydroxide Ethanedisulfonate: A Cationic Inorganic Layered Material for High-Capacity Anion Exchange*. Angew. Chem. Int. Ed. **2011**. 50, 9066 – 9070.

[26] Poudret, L., Prior, T.J., McIntyre, L.J., Fogg, A.M. *Synthesis and Crystal Structures of New Lanthanide Hydroxyhalide Anion Exchange Materials, $Ln_2(OH)_5X \bullet 1.5H_20$.* Chem. Mater. **2008**, 20, 7447-7453.

[27] Forster, P.M., Tafoya, M.M., Cheetham, A.K. *Synthesis and characterization of $Co_7(OH)_{12}(C_2H_4S_2O_6)(H_2O)_2$ – a single crystal study of a ferromagnetic layered cobalt hydroxide.* Journal of Physics and Chemistry of Solids. **2004,** 65, 11-16.

[28] Hindocha, S.A., McIntyre, L.J., Fogg, A.M. *Precipitation synthesis of lanthanide hydroxynitrate anion exchange materials, $Ln_2(OH)_5NO_3 \bullet H_2O$ (Ln = Y, Eu-Er).* Journal of Solid State Chemistry. **2009**, 182, 1070 – 1074.

[29] Gu, J-Z, Lu, W-G, Jian, L., Zhou, H-C, Lu, T-B. *3D Porous Metal-Organic Framework Exhibiting Selective Adsorption of Water over Organic Solvents*. Inorganic Chemistry. **2007**, 46, 5835 – 5837.